Citation: Ramos, A., Lopez-Mir, B., Wilson, E.P., Granado, P., Muñoz, J.A., 2020. 3D reconstruction of syn-tectonic strata deposited during the inversion of salt-related structures: insights from the Llert syncline (South-central Pyrenees). Geologica Acta, 18.20, 1-19.
DOI: 10.1344/GeologicaActa2020.18.20

geologica acta

3D reconstruction of syn-tectonic strata deposited during the inversion of salt-related structures: insights from the Llert syncline (South-central Pyrenees)

A. Ramos[1,2] **B. Lopez-Mir**[1,2] **E.P. Wilson**[1] **P. Granado**[1] **J.A. Muñoz**[1]

[1]**Institut de Recerca Geomodels, Departament de Dinàmica de la Terra i de l'Oceà Universitat de Barcelona**
C/ Martí i Franquès s/n, 08028 Barcelona, Spain. Ramos E-mail: adria_ramos@outlook.com.
Lopez-Mir E-mail: b.lopez@igme.es. Wilson E-mail: epwilson@ub.edu.
Granado E-mail: pablomartinez_granado@ub.edu. Muñoz E-mail: jamunoz@ub.edu

[2]**Instituto Geológico y Minero de España (IGME)**
Madrid, Spain

ABSTRACT

The Llert syncline is located in the South-central Pyrenees, between the eastern termination of the E-W trending Cotiella Basin and the north-western limb of the N-S trending Turbón-Serrado fold system. The Cotiella Basin is an inverted upper Coniacian-lower Santonian salt-floored post-rift extensional basin developed along the northern Iberian rift system. The Turbón-Serrado fold system consists of upper Santonian–Maastrichtian contractional salt-cored anticlines developed above an inverted transfer zone of the Pyrenean rift system. Based on field observations, we have conducted a 3D reconstruction of the Llert syncline in order to further constrain the transition between these oblique salt-related structures. Our results suggest that the evolution of the Llert syncline was mainly controlled by tectonic shortening related to the positive inversion of the Cotiella Basin, synchronously to the growth of the Turbón-Serrado detachment anticline. This structure was also conditioned by the pre-compressional structural framework of the Pyrenean rift system. Our contribution provides new insight into the geometric and kinematic relationships of structures developed during the inversion of passive margins involving salt.

KEYWORDS | **3D reconstruction. Cotiella Basin. Detachment anticlines. Salt tectonics. Tectonic inversion.**

INTRODUCTION

Salt-floored extensional systems associated with salt diapirs and listric faults are common in present-day continental margins such as offshore Angola (*e.g.* Brun and Fort, 2004; Cramez and Jackson, 2000; Fernandez *et al*., 2020), Equatorial Guinea (*e.g.* Tari *et al*., 2003; Turner, 1999), Brazil (*e.g.* Jackson *et al*., 2015; Mohriak *et al*., 2012), the Gulf of Mexico (*e.g.* Hudec *et al*., 2013; Salazar *et al*., 2014) or the SW Iberian margin (*e.g.* Ramos *et al*., 2017a, b, 2020). Owing to their economic importance to the oil industry, the structure of these salt-related extensional

systems has been extensively investigated through excellent 2D and 3D high resolution seismic imagery, combined with borehole datasets (*e.g.* Fernandez *et al.*, 2020; Mohriak *et al.*, 2012). However, uncertainties related to seismic imaging of salt-related structures limit the understanding of their 3D geometry and kinematics. In this sense, field analogues allow investigating features that are usually out of range of seismic resolution, helping to expand the ideas and concepts derived from seismic interpretation.

The Llert syncline in the South-central Pyrenees (Fig. 1) provides a unique opportunity to study in outcrop the relationships between two salt-related structures developed in the eastern part of the Bay of Biscay-Pyrenean Atlantic rift arm: the NW-SE trending Cotiella Basin and the N-S trending Turbón-Serrado fold system. The upper Coniacian-lower Santonian Cotiella Basin is a salt-detached extensional system consisting of several salt withdrawal minibasins bounded by diapirs, salt rollers and listric faults, which were subsequently inverted during the late Santonian-Maastrichtian onset of the Pyrenean Orogeny (Lopez-Mir *et al.*, 2016a). The syn-kinematic sedimentary infill is characterized by ramp carbonate sequences, which form sedimentary wedges thickening towards the SW, towards a presently inverted

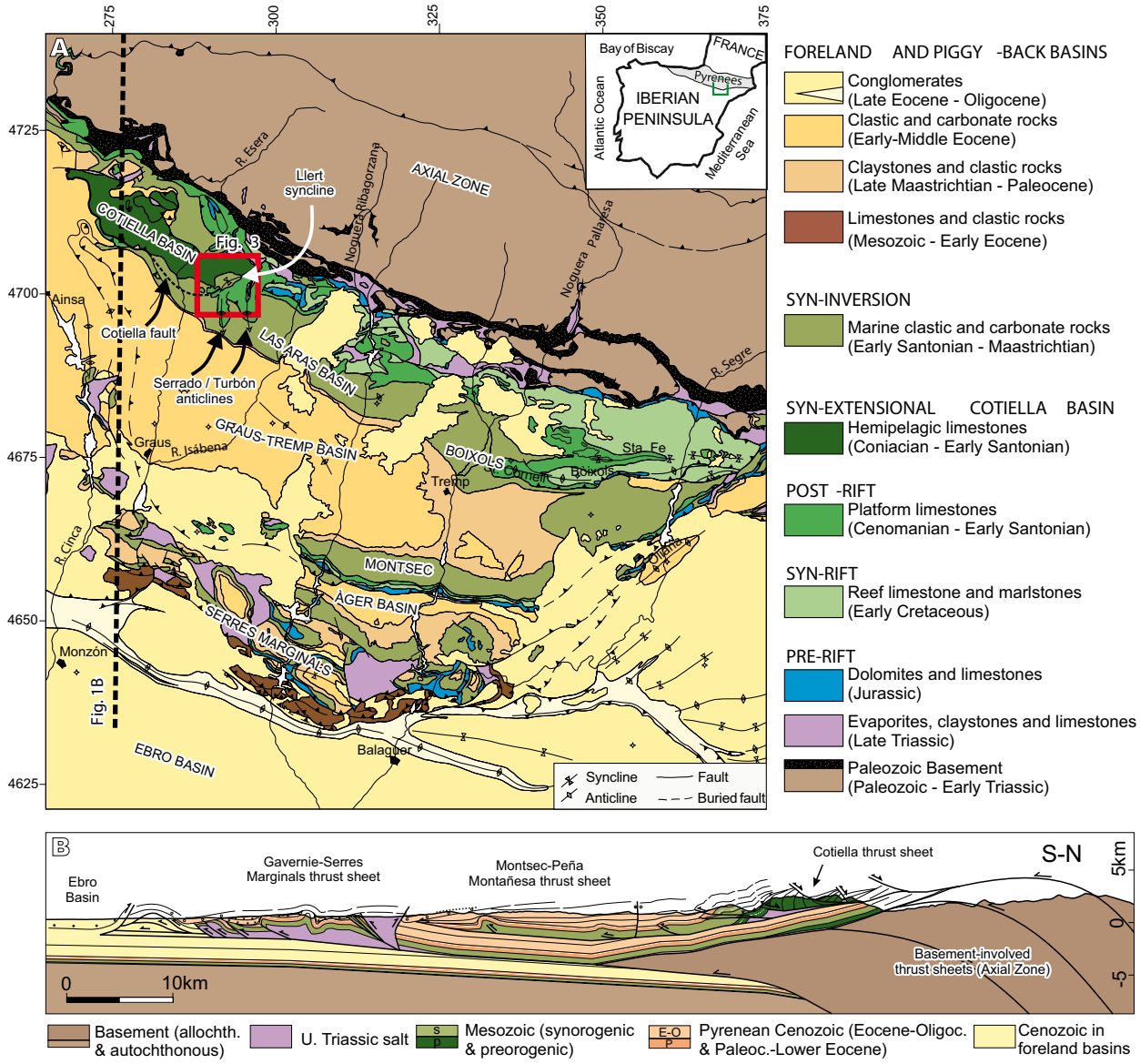

FIGURE 1. A) Geological map of the South-central Pyrenees indicating the main structural units (modified from Fernández, 2004; Muñoz *et al.*, 2018) and the location of the study area. The location of the map is represented by a green rectangle in the inset map at the top right corner. B) Regional cross-section showing the main structural elements along the western portion of the South-central Pyrenean thrust system (modified from Lopez-Mir *et al.*, 2016a).

basin-bounding extensional fault (McClay *et al.*, 2004). This fault exhibits a spoon-shaped geometry, characterized by a NE-dipping listric fault across most of the Cotiella Basin. However, in the study area the master fault dips to the NW, as the fault tips out NE of the Llert syncline (Lopez-Mir *et al.*, 2016a). Eastward the Cotiella Basin, the Turbón-Serrado fold system involves post-rift carbonate sequences significantly thinner (~300m) than the equivalent syn-kinematic sediments in the Cotiella Basin (~6km) (Lopez-Mir *et al.*, 2015). The Turbón-Serrado fold system is located in the footwall of the Cotiella extensional system, but also in the footwall of the Las Aras Lower Cretaceous syn-rift basin, located further east (Fig. 1) (García-Senz, 2002; García-Senz *et al.*, 2019a). Accordingly, all the major structures located in the study area show different orientations, from ESE-WNW (Las Aras and Cotiella Basins) to N-S (Turbón and Serrado anticlines), or NE-SW (Llert syncline). The connection between these structures and their relationships with the syn-kinematic and syn-orogenic sediments resulted into a complex three-dimensional (3D) framework, the understanding of which requires the use of 3D geological approaches.

This paper presents a 3D reconstruction of the Llert syncline. The 3D reconstruction was undertaken using existing 3D reconstruction methodologies developed in the Institut de Recerca Geomodels (Universitat de Barcelona) (*e.g.* Fernández *et al.*, 2004; Mencos *et al.*, 2015). These methodologies are designed to guide the extrapolation of surface or subsurface data to areas where data are scarce or missing, using geological constraints to minimize extrapolation uncertainties. Based on the availability and quality of field data, we applied different approaches, which enabled the use of geometrical models to constrain the subsurface structure. The main objective is to understand the connection between the Cotiella post-rift extensional basin and the highly oblique NS-trending Turbón-Serrado fold system in the footwall of the Las Aras Lower Cretaceous syn-rift basin. Our results provide a new insight into the kinematic evolution of the Llert syncline during the tectonic inversion of this area of the Pyrenean rift system.

GEODYNAMIC SETTING

The Pyrenees are a doubly verging Late Cretaceous to early Miocene orogenic system developed by the tectonic inversion of Mesozoic extensional basins in the southern branch of the Pyrenean rift system (Muñoz, 2002) (Fig. 1). Their geodynamic evolution is kinematically related to the opening of the Atlantic Ocean (Tavani *et al.*, 2018; Vergés and García-Senz, 2001), as detailed below.

Following the Variscan orogeny, an initial stage of late Permian-Triassic rifting culminated with the deposition of an Upper Triassic salt level (*i.e.* the Keuper facies), which was overlain by Lower and Middle Jurassic post-rift carbonate platforms (Fig. 2) (García-Senz, 2002). The main rifting event started at Late Jurassic to Early Cretaceous (Fig. 2). Major crustal thinning occurred from late Albian to Cenomanian times and was related to the opening of the central and North Atlantic Ocean. This led to the formation of large extensional basins and the exhumation of subcontinental mantle lithosphere, which culminated with accretion of oceanic crust in the westernmost Bay of Biscay (Jammes *et al.*, 2009; Roca *et al.*, 2011; Tavani *et al.*, 2018; Tugend *et al.*, 2014). The overlying upper Cenomanian to early Santonian strata is represented by carbonates, recording a period of thermal subsidence (Fig. 2). At this time, the development of post-rift carbonate platforms above thick Upper Triassic evaporites resulted into the development of passive-margin salt basins, such as the Cotiella Basin (Figs. 1; 2) (Lopez-Mir *et al.*, 2014, 2016a).

At the late Santonian, the onset of collision between the Iberian and Eurasian plates induced the inversion of the previous extensional basins (Fig. 2) and the development of Cotiella and Bóixols thrust sheets. Collision also led to the development of structural relief and adjacent foreland basins were characterized by strongly subsiding troughs in front of the inverted basins. These were filled by syn-orogenic deposits that grade forwards into carbonate platforms (García-Senz *et al.*, 2019a). Subsequently, during the Early Eocene to Oligocene, the Cotiella and Bóixols thrust sheets were transported tens of km southwards above the Montsec–Peña Montañesa and Gavarnie–Serres Marginals thrust sheets (Garrido-Mejías, 1973; Muñoz, 1992; Muñoz *et al.*, 2013, 2018; Séguret, 1972). In the study area, the tilting of these structural units towards the south (Fig. 1B) is related to the development of a later antiformal stack of basement-involved thrust sheets in the Axial Zone (Espurt *et al.*, 2019; Martinez-Peña and Casas-Sainz, 2003).

GENERAL STRUCTURE OF THE COTIELLA BASIN

The study area is located in the Cotiella-Bóixols thrust sheet, which is the upper structural unit of the South-central Pyrenees and was emplaced during the earliest stages of the Pyrenean Orogeny by the tectonic inversion of previous extensional basins (Berástegui *et al.*, 1990; Bond and McClay, 1995; García-Senz, 2002; Garrido-Mejías, 1973; McClay *et al.*, 2004; Muñoz *et al.*, 2013, 2018). The Cotiella-Bóixols thrust sheet developed from the tectonic inversion of the Lower Cretaceous rift basins located along the southern Pyrenean rift system margin (García-Senz, 2002; Saura *et al.*, 2016). This rift system was compartmentalized into different grabens with a stepped geometry, separated in cases by oblique (N-S) transfer

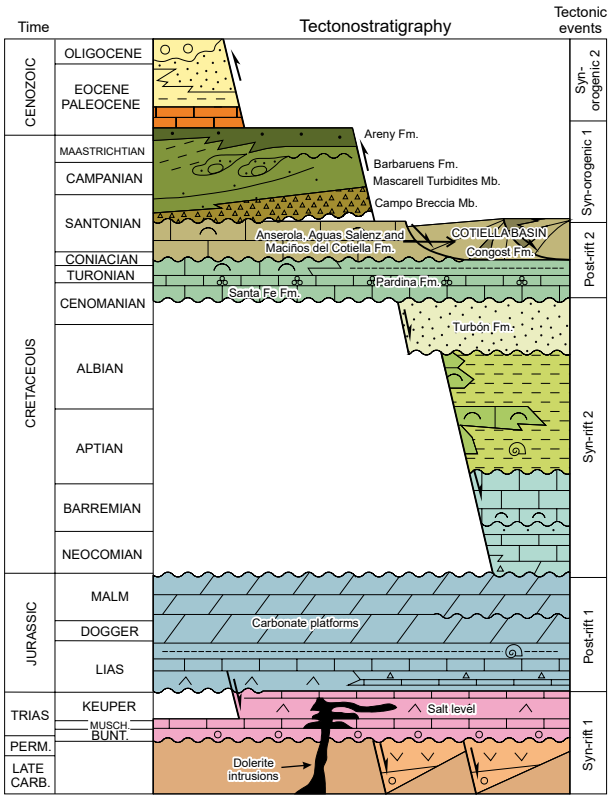

FIGURE 2. Chronostratigraphic diagram showing the stratigraphic units of the South-central Spanish Pyrenees and the tectonic events that controlled their deposition (modified from García-Senz, 2002; Lopez-Mir *et al.*, 2015).

faults. In particular, the Cotiella-Bóixols thrust sheet in the study area developed as a short-cut of the Lower Cretaceous Las Aras syn-rift basin, located farther east (Fig. 1). Here, the internal structure of the Cotiella-Bóixols thrust sheet consists of a transported detachment fold system, the most prominent elements of which are the NS-trending Turbón and Serrado anticlines, developed synchronously to the tectonic inversion of the Cotiella Basin. These folds are cored by the Upper Triassic evaporites and exhibit steep limbs, which delineate isoclinal profiles. The strong plunge towards the south (García-Senz, 2002) is related to the tilting by basement-involved underthrusting of the Axial Zone antiformal stack. Detachment folding was associated with the deposition of several km of slope sediments, with turbidites and resedimented carbonates onlapping the limbs of the growing anticlines (García-Senz, 2002) (Fig. 1). The anticlines are almost orthogonal to the NW-SE oriented trend of the Cotiella Basin (Fig. 1A).

The internal structure of the Cotiella-Bóixols thrust sheet consists of an upper Coniacian-lower Santonian salt-detached extensional system associated to prominent long-lived salt diapirs sourced from the Upper Triassic salt (Lopez-Mir, 2013, 2015, 2016a). In the hanging wall of the Cotiella thrust, the upper Coniacian-lower Santonian sediments reach up to 6km in their thickest interval. In the study area the hanging wall sediments are as much as 3km thick as the Cotiella fault tips out towards the NE. In the footwall of the Cotiella thrust, corresponding to the Turbón-Serrado fold system in the study area, the equivalent stratigraphic section is only ~300m thick and indicative of shallower depositional environments than the equivalent syn-kinematic sediments in the Cotiella Basin (García-Senz, 2002). Thus, the Turbón-Serrado fold system is located in the footwall of the Cotiella inverted extensional system, but also in the footwall of the Las Aras Lower Cretaceous syn-rift basin, located farther east (Fig. 1) (García-Senz, 2002; García-Senz *et al.*, 2019a). Positive tectonic inversion is recorded by the onlap of the syn-orogenic Campo Breccias Member and the related turbidites (García-Senz, 2002; McClay *et al.*, 2004), as detailed below.

The Llert syncline forms the connecting structure between the NW-SE trending inverted Cotiella Basin and the N-S striking Turbón and Serrado anticlines (Figs. 3; 4) and displays near vertical NE-SW-striking limbs. In detail, the north-western limb of the Llert syncline involves upper Coniacian to lower Santonian strata in the hanging wall of the partially inverted extensional listric Cotiella fault (*e.g.* Lopez-Mir *et al.*, 2015). In contrast, the south-eastern limb of the Llert syncline involves Jurassic to lower Santonian strata, in structural continuity with the western limb of the Turbón-Serrado anticlines (*i.e.*, in the footwall of the Cotiella fault). The structural framework of these Jurassic to lower Santonian strata at the subsurface is largely unconstrained since they are partially covered by upper Santonian to Campanian syn-inversion deposits.

STRATIGRAPHY

The stratigraphic succession exposed at the Llert syncline area has been simplified into pre-extensional, syn-extensional and syn-compressional sedimentary successions, depending to their timing of deposition with regards to the Cotiella fault activity. In the Turbón-Serrado area, the pre-extensional succession comprises a 300m thick succession of Jurassic post-rift carbonates, which directly overlay the Upper Triassic salt level (Fig. 2); these are unconformably overlain by ~200m of siliciclastic sediments of the late Albian to Cenomanian succession (Fig. 2). The base of the Turbón Sandstone Formation is an angular unconformity that marks the end of the Early Cretaceous rift event (Fig. 2). However, lower Cretaceous synrift sediments are absent in the study area (García-Senz, 2002).

The upper Albian to Cenomanian siliciclastic materials are followed by an upper Cenomanian to Coniacian carbonate

succession, which has been sub-divided into 3 formations of platform carbonates: the Santa Fe, Pardina and Congost formations (Caus *et al*., 1993; Gómez-Garrido, 1987; Mey *et al*., 1968; Robador and Zamorano, 1999) (Fig. 2). In the Cotiella Basin, the Jurassic succession is absent, while the Turbón Sandstones and the Cenomanian to Coniacian post-rift carbonates directly overlie the Upper Triassic salt. At outcrop, the thickness of the Cenomanian to Coniacian post-rift carbonates range from more than 750m in the Cotiella Basin (north-western limb of the Llert syncline) *(e.g.* Lopez-Mir *et al*., 2015) to a maximum of 500m in the Turbón-Serrado fold system (south-eastern limb of the Llert syncline) (*e.g.* García-Senz and Ramírez, 1997). These thickness changes can be considered insignificant when compared to the overlying upper Coniacian to lower Santonian stratigraphic succession, and so the Cenomanian to Coniacian post-rift carbonates are considered pre-extensional with regards to the Cotiella fault activity.

The overlying stratigraphic succession consists of three main formations (Maciños del Cotiella, Aguas Salenz and Anserola, Fig. 2), which are referred here to as the syn-extensional succession. The Maciños del Cotiella Formation (Misch, 1934) consists of upper Coniacian calcarenites with quartz and gravelly sandstones interpreted as sand bars deposited near the platform margin; it reaches a maximum thickness of 500m in the Baciero mountain range, corresponding to the north-western limb of the Llert syncline (Fig. 4), and 140m in the Turbón-Serrado fold system (*i.e.* south-eastern limb of the Llert syncline). Above, the Aguas Salenz Formation (Garrido-Mejías, 1973; Misch, 1934; Souquet, 1967) consists of a Coniacian to Santonian fine to medium-grained packstone with the foraminifera *Lacazina*, interpreted as slope and basin facies (Lopez-Mir, 2013). To the NW, in the Baciero mountain range (Fig. 4), the Aguas Salenz Formation reaches up to 1,100m, whereas to the SE in the Turbón anticline it is only 400m thick. In the centre of the Cotiella Basin, the succession consists of 6km of the Maciños del Cotiella and Aguas Salenz formations (García-Senz, 2002), indicating a significant stratigraphic expansion westward within the Cotiella Basin (Lopez-Mir *et al.*, 2014, 2015; McClay *et al.*, 2004). The Egea Formation consists of biohermal limestones interpreted as shallow platform limestones (Papón, 1969); it is approximately 45m thick and is found in the Collado de La Plana and Serrado anticline (west and south of Turbón Mountain, respectively; Fig. 3) interbedded with the Aguas Salenz Formation limestones. The Anserola Formation (Mey *et al.*, 1968) is composed of lower Santonian limestones, marly limestones and marls, deposited in an external platform to slope environment (Garrido-Mejías, 1973). The Anserola Formation reaches up to 480m in the north-western limb of the Llert syncline and 250m in the south-eastern limb, marking a decrease on extensional salt tectonic activity in the Cotiella Basin.

The syn-compressional strata record the onset of Pyrenean shortening during late Santonian to Maastrichtian times (Fig. 2) as recorded by a prominent EW-trending turbidite trough developed at the foreland of the evolving orogenic belt. Syn-compressional strata are bound by a basal unconformity, here referred to as the Campo unconformity (Fig. 5). In the study area, the syn-compressional succession is subdivided into the Campo Breccias and the Mascarell Turbidites members (Ardèvol *et al*., 2000; García-Senz, 2002; García-Senz *et al*., 2019b; Garrido-Mejías, 1973; Robador and Zamorano, 1999; Souquet, 1967; van Hoorn, 1970). The Campo Breccias Member consists of limestone breccias alternating with thinly-bedded sandy turbidites, which onlap the Campo unconformity (Fig. 5) (Robador and Zamorano, 1999). According to van Hoorn (1970), the breccias contain boulders of limestones with Coniacian-Santonian foraminifera, and limestones belonging to the Pardina and Aguas Salenz formations, indicating a source area located in the emerging Cotiella Basin. Additional boulders of limestones with orbitolinids of the Aulet Formation (Souquet, 1967), and diabase and Permian-Triassic green and red clays indicate a contribution from another source area located in the Pyrenean rift basins or beyond (García-Senz, 2002; McClay *et al*., 2004; Robador and Zamorano, 1999). At outcrop scale, the Campo Breccias Member reaches a maximum thickness of 180m in north-western limb and 110m in the south-eastern limb of the Llert syncline. The overlying Mascarell Member (part of the Vallcarga Formation) consists of an upper Santonian-Campanian turbidites and marls (Lagier, 1985; Nagtegaal, 1972; Souquet, 1967), which record some incipient tectonic activity in the area. García-Senz and Ramírez (1997) documented a maximum thickness of 650m for this member in the Las Vilas syncline, located immediately east of the Turbón anticline. Compositional analyses of the Vallcarga turbidites by van Hoorn (1970) show that they are largely built up of intrabasinal calcareous material, including rock fragments derived from an intrabasinal erosion of Mesozoic formations found at the base of the formation. Based on the dimensions of the Vallcarga basin, too small to permit a great flow distance, van Hoorn (1970) interprets that all the turbidites were deposited rather proximal to the source area.

DATASETS AND METHODOLOGY

In this work, we have followed a method based on the implementation of geological limitations to interpolate between data and extrapolate beyond them. An effective way to reconstruct 3D surfaces by implementing structural geology criteria is through contour mapping. Structural contours are isolines, representing horizontal lines separated by the same value of z (depth or altitude); therefore, contour maps are topographic maps of surfaces (Groshong, 2006).

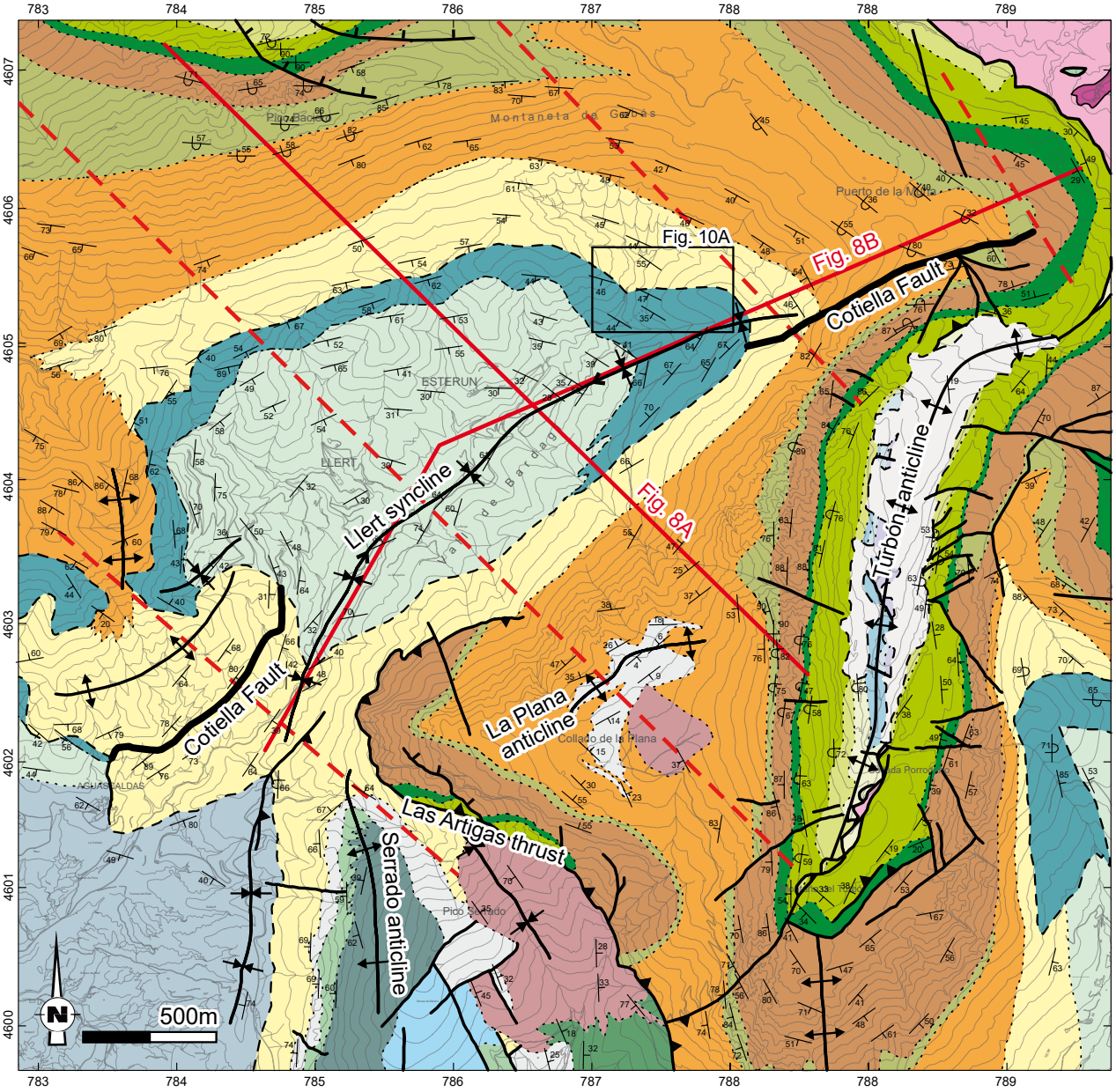

FIGURE 3. Geological map at 1:5,000 scale of the study area, indicating the location of the cross-sections (in red) and the structural data used for the 3D tructural reconstruction. The location of the 6 cross-sections built for 3D model construction are represented by straight red lines (the continuous ones are shown in detail in Fig. 8). This map compiles all of our data and includes the information from previous (García-Senz and Ramírez, 1997; Lopez-Mir, 2013; Robador and Zamorano, 1999).

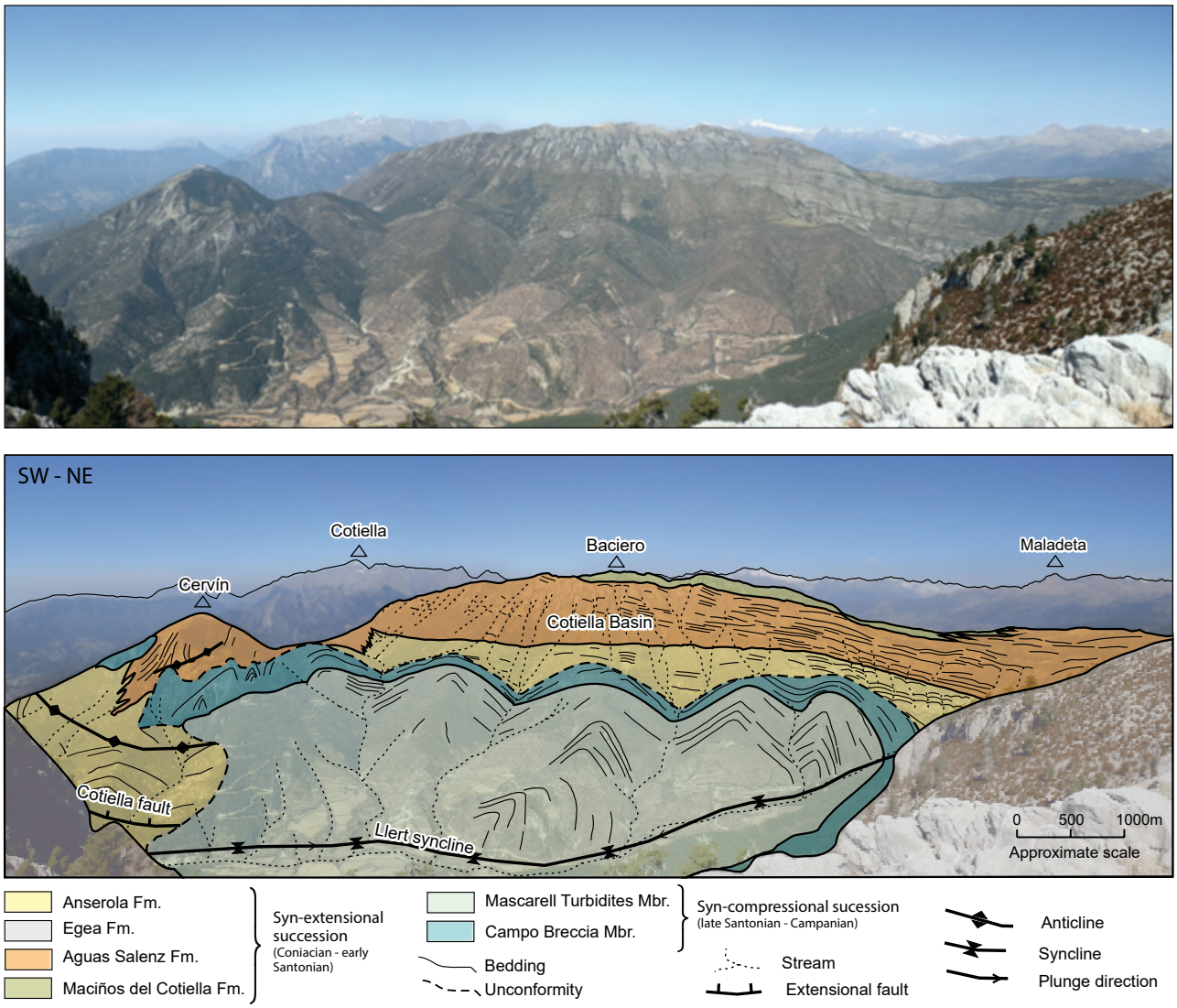

FIGURE 4. View of the NW limb of the Llert syncline from La Plana del Turbón. The core of the syncline exposes upper Santonian-Campanian syn-compressional sediments, which unconformably overlay upper Coniacian-lower Santonian sediments of the Cotiella Basin.

The workflow consists of four main steps: data acquisition, 3D digitalization, structural analysis and 3D reconstruction (Fig. 6).

The 3D model presented in this paper was largely built from structural and stratigraphic data collected in the field, including a 1:5,000 geological map of the study area and more than 200 dip measurements. Two geological maps at 1:50,000 of Pont de Suert and Campo (García-Senz and Ramírez, 1997; Robador and Zamorano, 1999, respectively) and a 1:25,000 geological map of the Cotiella thrust sheet (Lopez-Mir *et al.*, 2016b), were also used for the 3D reconstructions. The surface data-based 3D geological model of the Cotiella thrust sheet by Lopez-Mir *et al.* (2016a) and an unpublished seismic data-based 3D geological model of the Tremp-Graus basin (Fernández, 2004; Muñoz *et al.*, 2000), were used to constrain the subsurface structure.

The main goal of the 3D digitalization step is transferring and analysing the data into a 3D environment, in order to optimize the available geological data. For instance, there are numerous *in-house* computer tools to extract additional geological information such as the punctual dip of 3D map traces (Fernández, 2004) or the stratigraphic distance between horizons (Groshong, 2006). To this end, the construction of an accurate Digital Terrain Model (DTM) is essential (Fig. 7A). This includes the construction of a Triangulated Irregular Network (TIN) and a regular mesh (LATTICE) using vector topographic maps, which are then draped by orthophotographs (Fig. 7A; see Mencos, 2011). In this study, 3D digital mapping was carried out taking

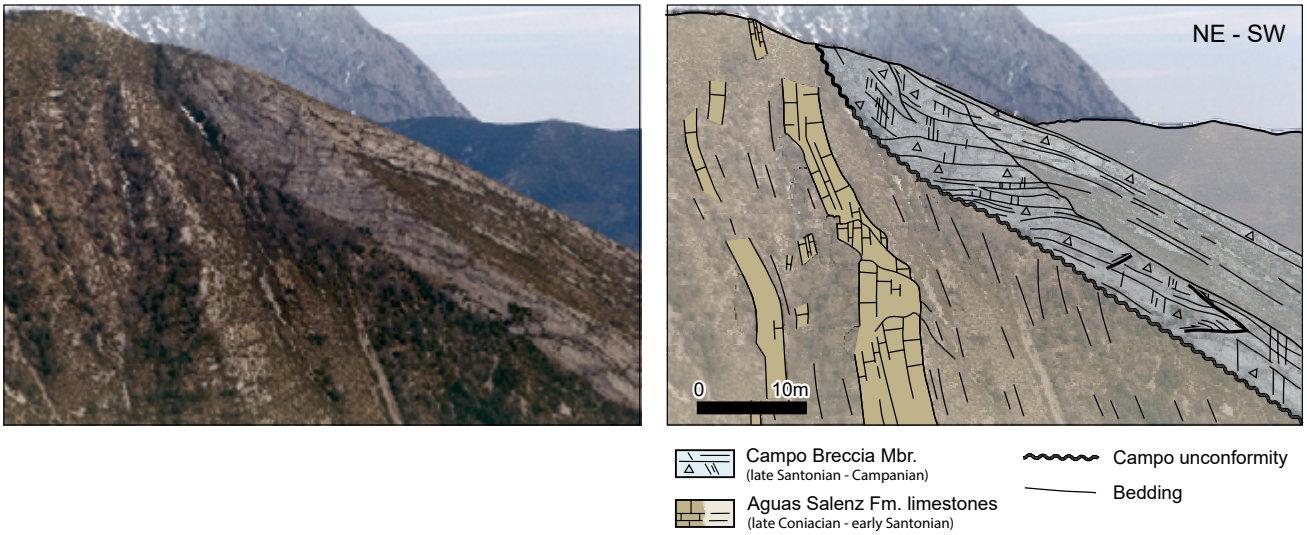

FIGURE 5. Detail of the Campo unconformity and the onlap of the Campo Breccias on the Aguas Salenz Formation in the Sierra del Cervín. View is from the north-west. Modified from García-Senz (2002).

into account georeferenced orthophotographs of the study area with a 0.5x0.5m pixel size (made available by the *Sistema de Información Territorial de Aragón* – SITAR; https://boletinagrario.com/f296,sitar-sistema-informacion-territorial-aragon.html) and 3D topographic maps at scale 1:5,000 (also provided by SITAR). The error of this process is about +/- 5m regarding the original information due to the resolution of the DTM mesh.

The following structural analysis and the 3D reconstruction steps are interrelated, since the 3D reconstruction methodology will mainly depend on the type of structural analysis performed. The main goal is to integrate the available data into a 3D geometrical representation of each geological surface. Depending on the type and amount of available data, three main methodologies were used: i) contour mapping following a dip-domain approach; ii) contour mapping aided by surface traces and iii) interpolation between cross-sections (Carrera *et al.*, 2009; Fernández *et al.*, 2004; Lopez-Mir *et al.*, 2016a; Mencos *et al.*, 2015; Snidero *et al.*, 2011).

Geological surfaces with a continuous trace and plenty of direct dip measurements were reconstructed through contour mapping following a dip-domain approach (Fernández *et al.*, 2004). The constructed geological surfaces represent the syn-orogenic strata, including the Campo unconformity (base of the Campo Breccias Member) and the base of the Mascarell Turbidites Member. The dip-domain method assumes that geological structures can be sub-divided into a finite number of planar dip-domains bounded by axial surfaces, faults or stratigraphic discontinuities (Fernández *et al.*, 2004; Groshong, 2006). However, when beds are not parallel the axial surfaces between dip-domains are not bisectors. To avoid mistakes derived from the angularities between beds, the tolerances and the boundary conditions for the 3D reconstruction of growth strata were very carefully fixed (*i.e.* 10º for the azimuth and the dip) and the geological surfaces were constructed one by one, rather than using a reference surface (*i.e.* a chosen horizon that accumulates as much data as possible, from which the rest of the surfaces will be reconstructed by means of applying stratigraphic thicknesses). The structural analysis of data

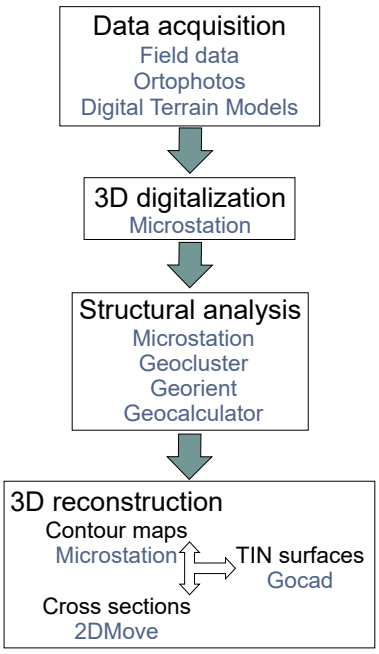

FIGURE 6. Workflow for the 3D reconstruction of the Llert syncline, showing the data and software used. TIN: Triangulated Irregular Network.

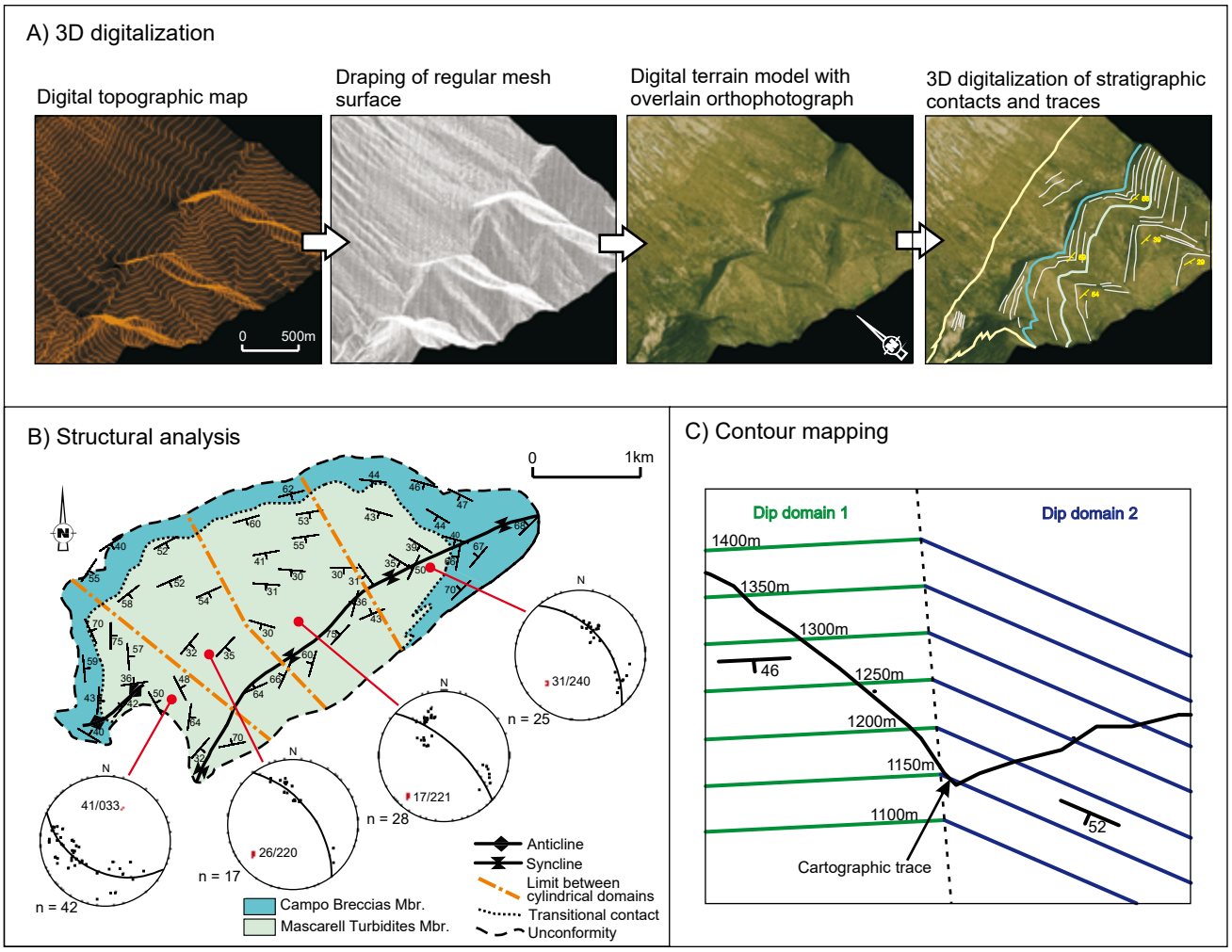

FIGURE 7. A) DTM construction process, superposing different types of data. B) Structural analysis of the syn-inversion turbidites coring the Llert syncline, resulting in four cylindrical dip-domains. C) Isoline construction using two constant dip domains and the position of the cartographic trace.

from the syncline core also allowed the determination of up to four cylindrical domains (Fig. 7B); the corresponding plunge lines (defined as the stereonet major circle of each cylindrical domain) were used as additional constraints for contour mapping (Fig. 7C).

In areas where dip-data was scarce it was not possible to define dip-domains, and then two different 3D reconstruction approaches were used. Geological surfaces with little dip-data but a continuous trace were reconstructed through contour mapping aided by the position of surface traces (Fig. 7C). These surfaces consist of faults that were reconstructed individually, applying additional geological constraints when required (*e.g.* fault-bend-fold models).

In contrast, geological surfaces with a discontinuous trace outcrop and few direct dip measurements were reconstructed following a 2D ½ construction approach, based on interpolation between cross-sections. These surfaces correspond to the ones located underneath the Campo unconformity (*i.e.* Anserola, Aguas Salenz and Maciños del Cotiella stratigraphic units) and accordingly buried by the syn-orogenic deposits. To this end, six cross-sections were built taking into account field data and the geological maps (Figs. 8; 9). The cross-section construction and interpolation methodologies are outlined below, since these were used as main constraints to reconstruct the sub-surface structure.

The cross-sections integrate the few available dip data, as well as stratigraphic thicknesses documented by Martín-Chivelet *et al.* (2019), after García-Senz (2002) and Lopez-Mir (2013). To interpret the structure at the subsurface, the top of the Anserola Formation was constructed using the Campo unconformity as reference horizon (Fig. 10). Since strata are not parallel, an angular relationship between the Anserola and Campo Breccias was calculated from the geological map in

Figure 3. Each calculation was based on the length of the map traces (measured from the point where they onlap the unconformity to a certain point of the same trace), and on the stratigraphic thickness between the unconformity and the trace (measured at the same point of the trace) (Fig. 10). Then, the calculated angle was used to construct the base of the Anserola Formation at an angle to the Campo Breccias Member surface. The stratigraphic surfaces below (i.e. the bases of the Aguas Salenz and Maciños del Cotiella stratigraphic units) were constructed assuming that: i) the Aguas Salenz and Maciños del Cotiella in the hanging wall of the Cotiella fault expand towards the fault and ii) the thickness of the Aguas Salenz and Maciños del Cotiella in the footwall of the Cotiella fault experiences much less variations than the hanging wall (Fig. 8). These assumptions are geologically reasonable based on the regional geology and the common understanding of salt-detached growth faults (*e.g.* Brun and Mauduit, 2008). In such way, the Aguas Salenz and Maciños del Cotiella stratigraphic units were constructed using the base of the Anserola Formation as the reference horizon, using the angular relationships observed in the map as geological constraints for the Cotiella fault hanging wall, and considering parallel beds in the footwall (Fig. 8).

The pre-extensional formations (i.e. Turbón Sandstone, Santa Fe, Pardina, Congost), were reconstructed using the base of the Maciños Formation as a reference horizon, assuming that the underlying layers were parallel to one another both in the footwall and the hanging wall of the Cotiella fault (Fig. 6). The truncation of the Jurassic successions at the eastern limb of syncline by the angular unconformity at the base of the Turbón Sandstone Formation (Fig. 6) is based on the field observations and interpretations by García-Senz (2002). The pre-extensional stratigraphic units are only depicted in the cross-sections since there was not enough data to constrain their 3D geometry. The geometry of the Cotiella fault at the subsurface is interpreted by Lopez-Mir (2013) and Lopez-Mir *et al.* (2016a). The interpretation of the Bóixols Thrust position under the Llert syncline is supported by previous works in the study area (Fernández, 2004; García-Senz, 2002; López-Mir, 2013) (Fig. 6). In summary, 3D reconstructions of the following geological surfaces are presented: the Cotiella fault and the bases of the Mascarell Turbidites, Campo Breccias, Anserola, Aguas Salenz and Maciños del Cotiella stratigraphic units.

3D GEOMETRY OF THE LLERT SYNCLINE

In map-view, the Llert syncline consists of two limbs, which are roughly 5km long and are oriented SW-NE (Figs. 3; 4). Both limbs are near-vertical (García-Senz, 2002) and the north-western limb is locally overturned (Figs. 3; 8). These limbs meet at the NE and the SW ends of the syncline and, as a result, the syncline exhibits a bowl-like basin geometry, characterised by a doubly-plunging fold axis (Figs. 3; 4; 8). The core of the syncline consists of the syn-compressional upper Santonian to Campanian stratigraphic succession, the base of which forms the Campo unconformity.

Above the Campo unconformity, the upper Santonian to Campanian strata of the Campo Breccias Member thicken towards the centre of the Llert syncline, reaching a maximum thickness of 275m (Fig. 8A). The breccias onlap the Campo unconformity at both limbs of the syncline (see Fig. 5 for onlap geometries of Campo Breccias Member over the Aguas Salenz Formation to the Cotiella Basin). This suggests that both the Turbón anticline and the inversion of the Cotiella Basin were synchronous to the deposition of the syn-compressional sediments. Moreover, the paleocurrents in the Campo Breccias Member and the Mascarell Turbidites Member have a NE-SW direction (van Hoorn, 1970; García-Senz, 2002). These are parallel to the syncline axis, which suggests a certain degree of confinement of the syn-compressional sediments currents during the deposition. Towards the S and SE, the Mascarell Turbidites Member directly onlap the Campo unconformity (García-Senz, 2002), suggesting a syntectonic behaviour during the development of the Llert syncline.

The sediments above the Campo unconformity (*i.e.* Campo Breccia and Mascarell Turbidites) cover both the Cotiella fault and the pre-compressional strata at the centre of the syncline (Figs. 3; 4; 8; 11; 12). As a result, the Cotiella fault is only exposed to the NE and SW of the Llert syncline, where the fold axial trace intersects the Campo unconformity (Figs. 3; 4). Where exposed, the Cotiella fault dips about 50º to the NW and is broadly parallel to the syncline axial trace (Fig. 3). Such orientation is interpreted to continue underneath the Campo unconformity, separating the pre-compressional strata of the north-western limb from the south-eastern limb (Fig. 8), as detailed below.

The north-western limb of the Llert syncline underneath the Campo unconformity exposes up to 4.8km of upper Coniacian to lower Santonian strata (Fig. 8), which are in structural continuity with the Cotiella Basin. At the syncline centre, these strata are buried by syn-compressional sediments (Figs. 3; 8). Upper Coniacian to lower Santonian sedimentary wedges expanding towards the Cotiella fault. The equivalent stratigraphic units in the Cotiella Basin have been interpreted to be indicative of syn-sedimentary salt tectonic activity and gravity-driven extension (Lopez-Mir *et al.*, 2014, 2015) (Figs. 11; 12).

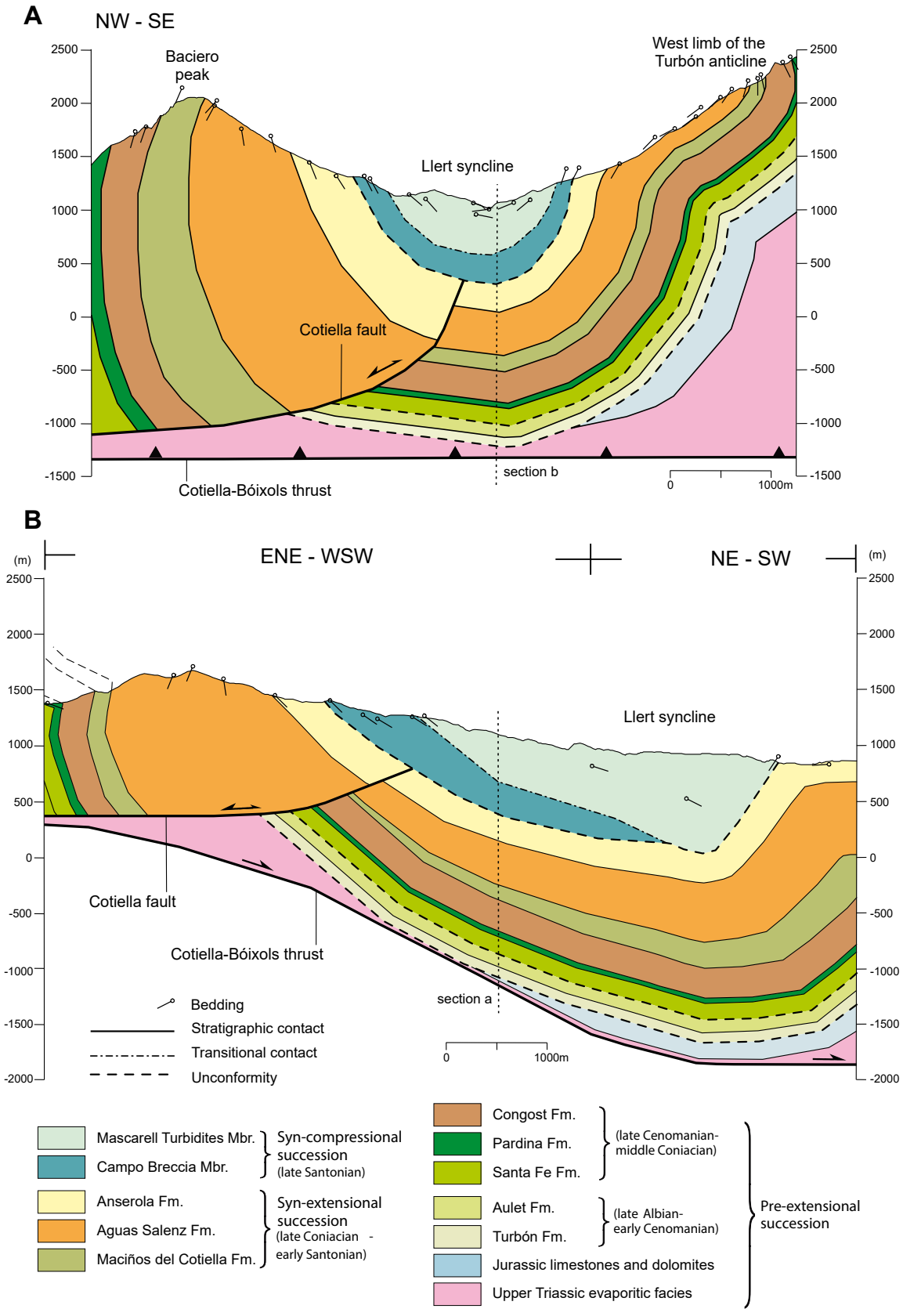

FIGURE 8. Two cross sections A) across strike and B) along the Llert syncline. These cross-sections are the most well-constrained and representative of the Llert syncline structure. See Figures 3 and 9 for location.

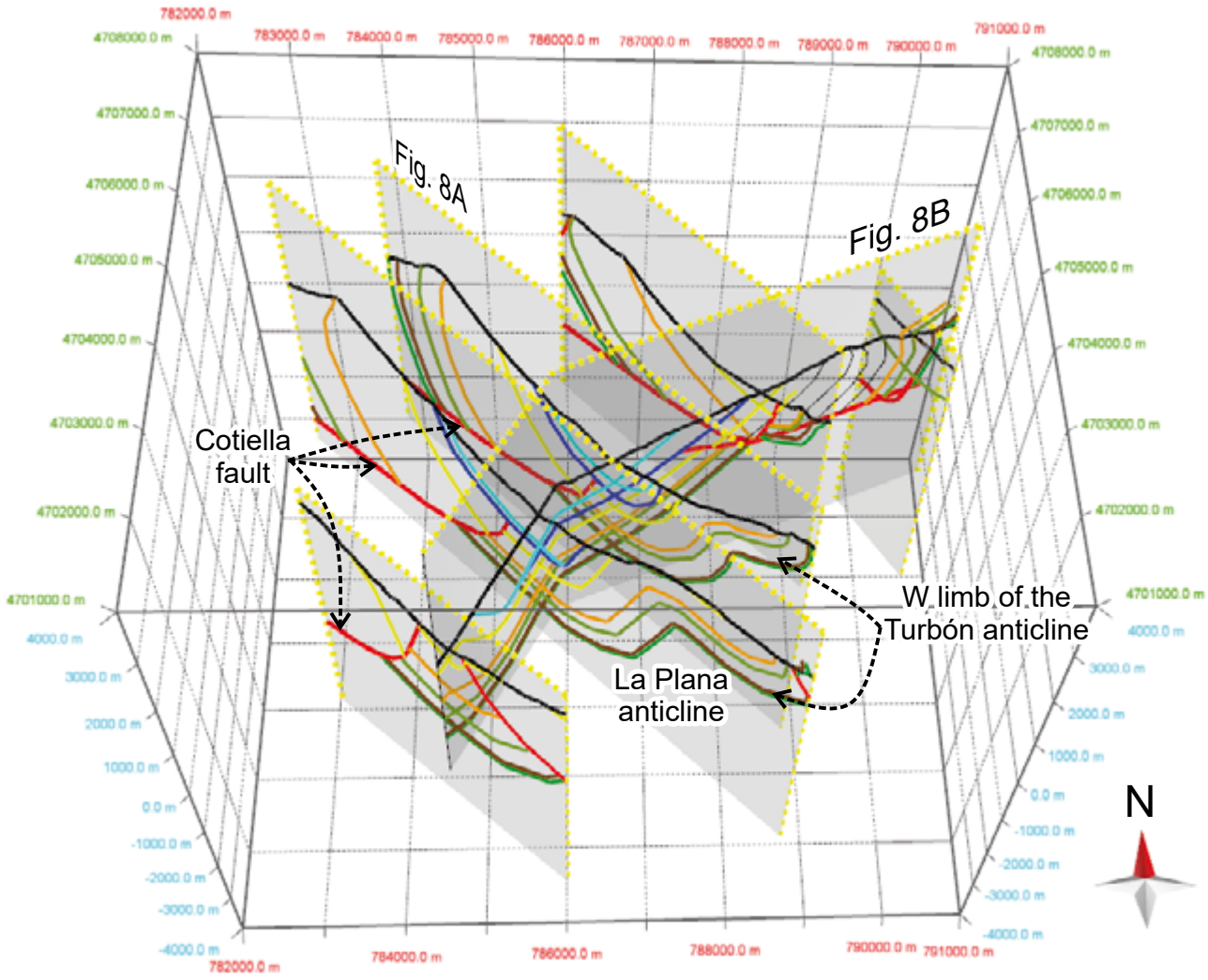

FIGURE 9. North-looking 3D view of six cross-sections along and across-strike of the Llert syncline. These sections were the framework for the 3D model presented throughout this paper.

For simplicity, our 3D reconstruction assumes that the thickness of the Coniacian to lower Santonian succession at the syncline centre remains constant. It directly overlies the Upper Triassic salt, while Jurassic to lower Cretaceous sediments are largely absent (García-Senz, 2002; Lopez-Mir *et al.*, 2014; McClay *et al.*, 2004). This succession is significantly thinner in the south-eastern limb than the equivalent succession in the north-western limb. The only noticeable thickness variation occurs in the Aguas Salenz Formation, which expands towards the Cotiella Basin, and in the Jurassic strata, which are truncated by the angular unconformity at the base of the Turbón Sandstone Formation (Figs. 8; 11; 12). This unconformity responds to the unconformably overlying sediments on top of a faulted and tilted margin, postdating rifting (García-Senz, 2002).

Farther to the east, the transition between the south-eastern limb of the Llert syncline and the Turbón-Serrado fold system occurs along a number of second-order NE- to N-trending folds (Figs. 3; 4). In general, these are contractional folds developed as hanging wall salt-cored anticlines above second-order thrusts and are made up of near-vertical to overturned limbs (Fig. 3). The most prominent of these structures is the Collado de La Plana anticline, located in the hanging wall of a W- to SW-directed thrust (García-Senz, 2002). Second-order thrusts revealing contractional deformation are also exposed at the north-eastern tip of the Cotiella fault. They affect pre- and syn-extensional strata at the footwall of the Cotiella Basin, corresponding to the north-western limb of the Turbón anticline (Fig. 3), and were likely developed during the Cotiella Basin tectonic inversion.

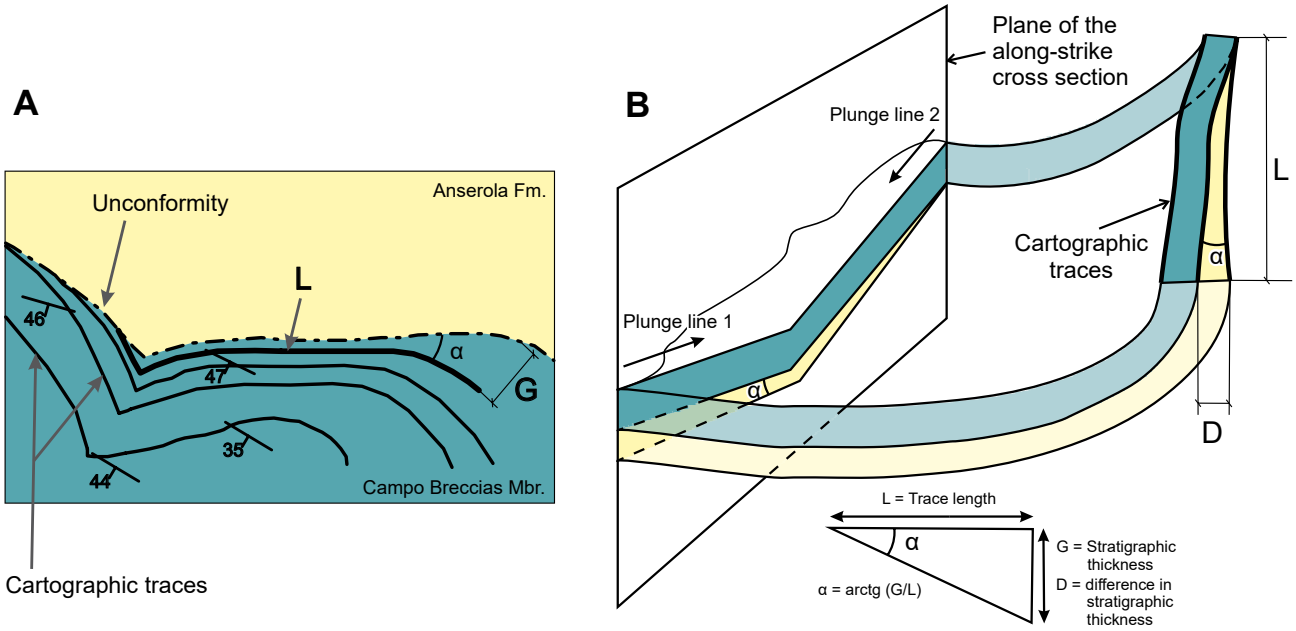

FIGURE 10. Method to calculate the onlap angle of the Campo Breccia Member over the unconformity. A) Portion of the Llert syncline in map view. See Figure 3 for location. B) 3D schematic reconstruction of the Cotiella fault footwall at depth, where α is the angle between two stratigraphic units calculated from the difference in stratigraphic thickness between different points of its outcrop trace. This angularity is assumed to be constant in depth and along a longitudinal section, and accordingly it was added to the dip data in both limbs of the Llert syncline to construct the syn-compressional contacts at depth.

EVOLUTION OF THE LLERT SYNCLINE

Our interpretation suggests that the kinematic evolution of the Llert syncline was controlled by two main evolutionary stages (Fig. 13): i) development of the salt-detached Cotiella fault during the Coniacian to early Santonian; ii) development of the Turbón anticline and the Llert syncline during the late Santonian–Maastrichtian shortening.

In the first evolutionary stage, the Cotiella fault is considered to develop along an uplifted, eroded and faulted rift margin. The erosion of the Jurassic sequences at the rift shoulder, possibly also related to salt inflation, resulted in the deposition of the late Coniacian to the early-Santonian Cotiella strata directly above the Upper Triassic salt level (Fig. 12A) (McClay *et al.*, 2004). In the Cotiella fault hanging wall, the expansion of strata towards the Cotiella fault is reasonable with the tectonic model presented by Lopez-Mir *et al.* (2015, 2016a), in which salt evacuation would have been coeval to post-rift gravity-driven extension, creating additional accommodation space for the deposition of thick sequences of syn-extensional growth strata (*e.g.* Cotiella Basin in Fig. 13A). East of the Cotiella fault (*i.e.* the fault footwall), the much thinner equivalent syn-extensional growth strata show little thickness variations so that they were not affected by salt tectonics (Fig. 13A). The absence of Jurassic sediments in the eastern limb of the Turbón anticline (Fig. 3) is interpreted to be controlled by a N-S trending extensional fault (Fig. 13), which coincides with the location of the anticline axial plane and is in turn related to a relay ramp of the Pyrenean rift system.

In the second evolutionary stage (Fig. 13), the growth of the Turbón-Serrado detachment anticlines during late Santonian-Maastrichtian shortening was determined by the pre-compressional salt tectonic framework and, in particular, by the occurrence of relay ramps of the Pyrenean rift system (*e.g.* García-Senz, 2002). This relay ramp system would connect the western tip of the Las Aras syn-rift extensional fault with another basin-bounding extensional fault located to the northwest. To the west, late Santonian-Maastrichtian shortening uplifted and inverted the salt-related depocenters of the Cotiella Basin. These two processes generated two structural highs, separated by a synformal trough (*i.e.* Llert syncline), which was filled by material partially sourced from the surrounding uplifted areas (Fig. 13B). This is recorded by the onlap relationships and the occurrence of immature clasts sourced from the Coniacian to middle Santonian successions within the Campo Breccia. The orientation of the Campo Breccia and the Mascarell stratigraphic units in the north-western limb of the

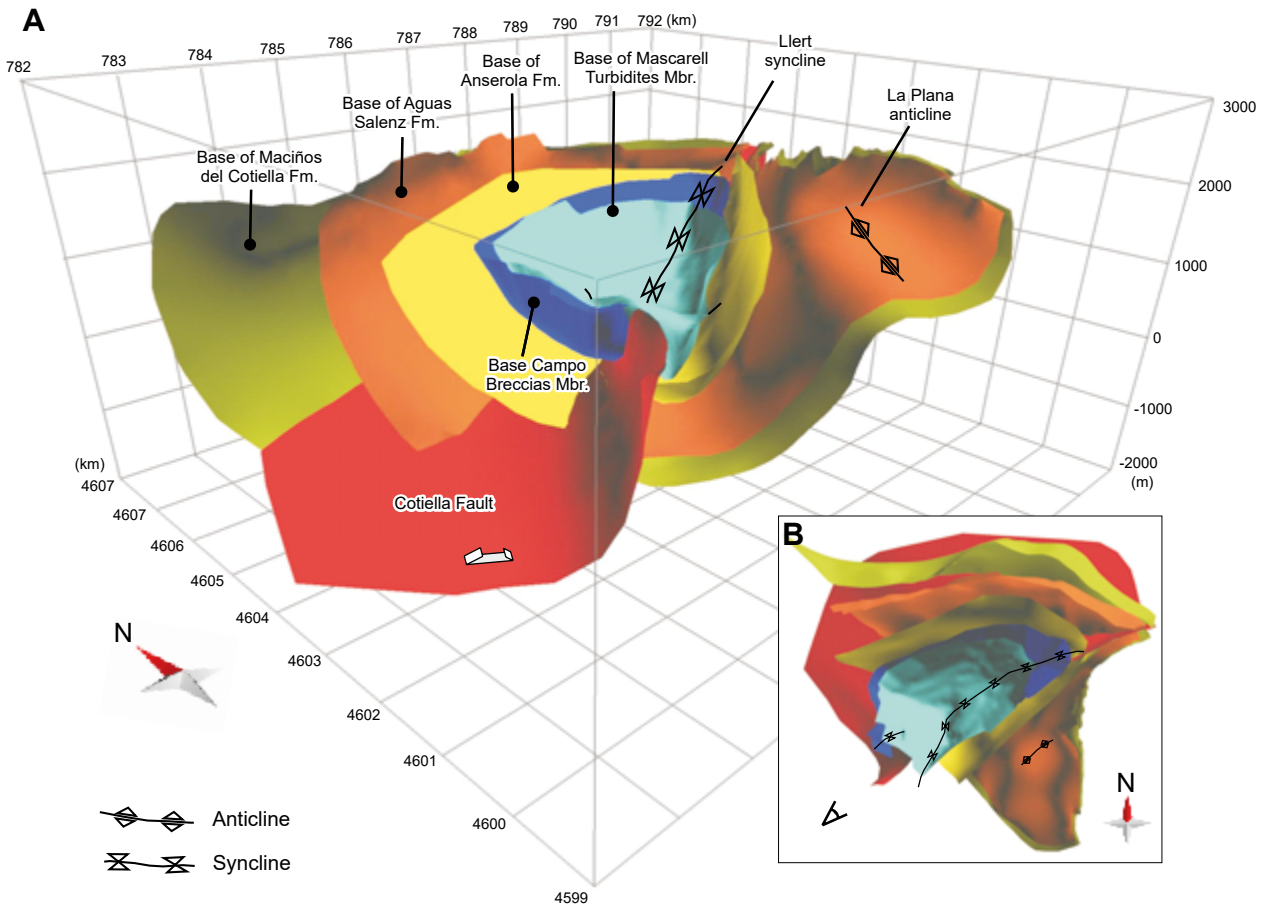

FIGURE 11. A) 3D structural model, seen from the SW. B) Plan view of the Llert syncline.

syncline coincides with that of the tilted EW-trending Cotiella Basin; whilst the orientation of the eastern limb of the syncline coincides with that of the western limb of the NS-trending Turbón anticline (Figs. 3; 8A). The syncline developed synchronously to the onset of the southerly-directed Cotiella and Bóixols thrust (Fig. 13B). Accordingly, we interpret that the development of the Llert syncline is intimately related to the growth of structural relief in two areas with strongly oblique structural trends during the onset of Pyrenean shortening.

CONCLUSIONS

The Llert syncline exhibits a tight geometry characterized by near-vertical limbs. The north-west limb is in structural continuity with the inverted Cotiella Basin, while the south-east limb is in structural continuity with the Turbón-Serrado fold system. The syncline shows a bowl-like basin geometry, with a doubly-plunging fold axis. The Cotiella fault shows a listric geometry dipping towards the northwest and is parallel to the Llert syncline axial trace. The fault is buried beneath the syn-compressional sediments, separating the pre-compressional succession of the north-western limb from the south-eastern limb. This is supported by a new 3D reconstruction of the Llert syncline, which demonstrates the continuity of the surrounding structures in the sub-surface.

The most relevant conclusions regarding the evolution and the tectonic style of the Llert syncline are summarized below:

i) The Llert syncline developed during the late Santonian to Maastrichtian times as a result of the tectonic inversion of the Cotiella salt basin to the west synchronously to the growth of the Turbón-Serrado detachment anticlines to the east.

ii) The tectonic inversion event was largely recorded by the deposition of the syn-compressional sediments in the core of the syncline, which were sourced

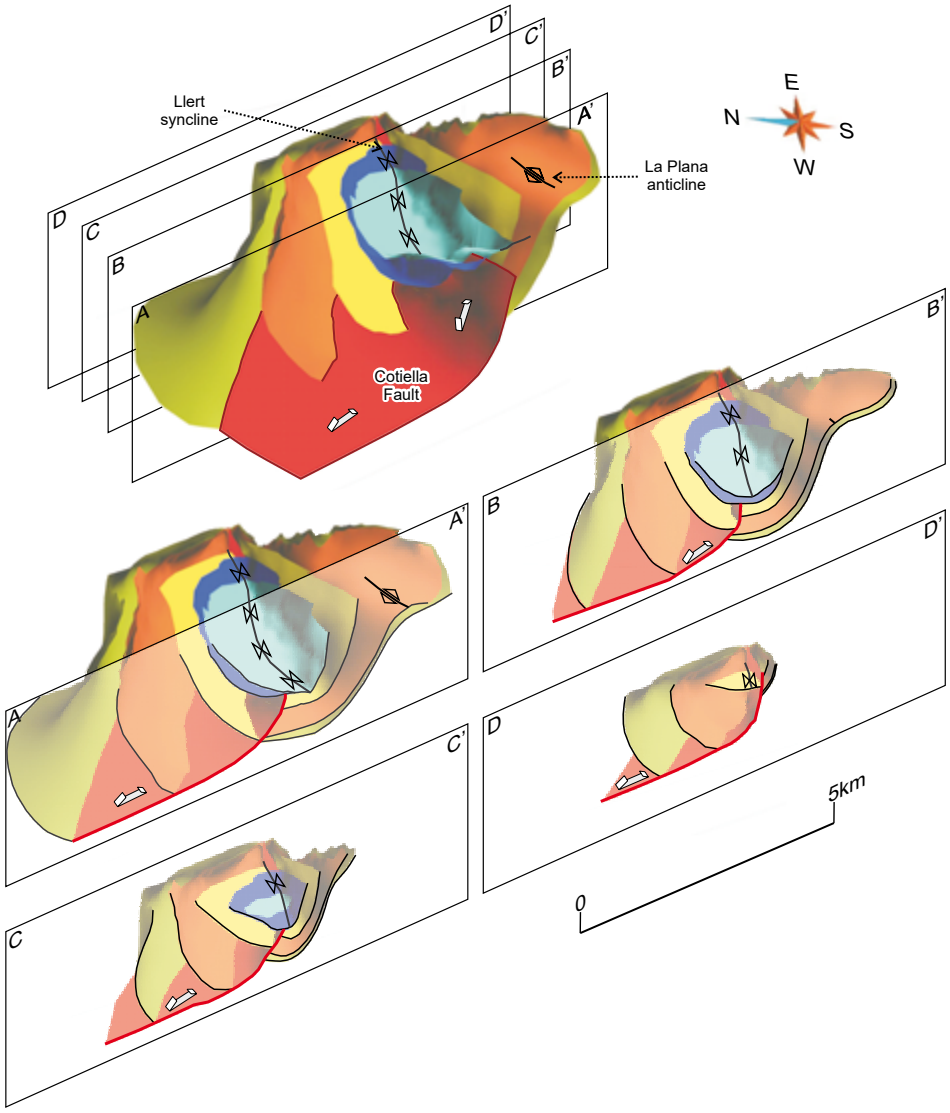

FIGURE 12. 3D Structural model of the Llert syncline (seen from the west) and vertical slices trending NW-SE, perpendicular to the Cotiella fault trend, showing the easternmost termination of the Cotiella fault. The colour codes of the different horizons are detailed in Figure 8.

from the surrounding uplifted areas. Changes on the sedimentary architecture of the post-rift succession and on the distribution of the Upper Triassic salt level, likely related to the configuration of the previous Pyrenean rift System, allowed the development of the Turbón salt-cored detachment anticline during shortening.

ACKNOWLEDGMENTS

This is a contribution of the Institut de Recerca Geomodels, Universitat de Barcelona. The authors acknowledge financial support from the Ministerio de Ciencia e Innovación "Proyecto INTECTOSAL, CGL2010-21968-C02-01" and "Proyecto SALCONBELT CGL2017–85532-P MINECO/FEDER, UE" and the Generalitat de Catalunya (Grup de Recerca de Geodinàmica i Anàlisi de Conques 2009SGR1198, 2001SRG-126 000074 and 2014SGR467SGR). Research by B. Lopez-Mir was funded by the predoctoral grant Formación del Profesorado Universitario from the Ministerio de Educación, Cultura y Deporte. This research was also carried out with the financial support of REPSOL, STATOIL and OMV Exploration and Production GmbH. Midland Valley (now Petroleum Experts), Paradigm and Bentley Systems are thanked for providing academic licenses of Move™, GoCAD™ and Microstation™ software, respectively. The authors also wish to thank Antonio Teixell, Antonio Casas and Juan Ignacio Soto for their helpful reviews.

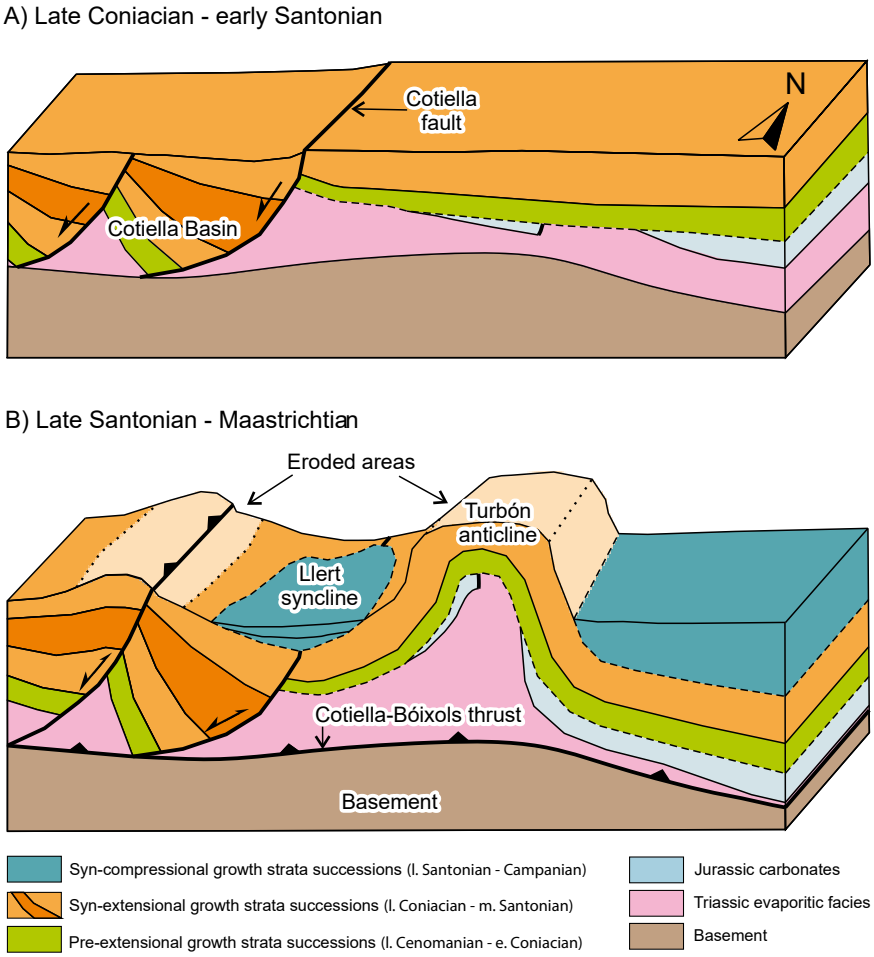

FIGURE 13. Sketched geological model showing the main stages of evolution of the Llert syncline from the late Coniacian-early Santonian to the late Santonian-Maastrichtian. A) Development of a listric growth fault detached on Upper Triassic salt. Notice the syn-rift extensional faults in the footwall of the Cotiella fault, along with the tilting to the east of the entire extensional system. B) Development of the Llert syncline during shortening related to early Alpine compression. Notice that the syncline is filled by sediments sourced by surrounding eroded areas (*i.e.* the Turbón detachment anticline and the inverted Cotiella Basin.

REFERENCES

Ardèvol, L., Klimowitz, J., Malagón, J., Nagtegaal, P.J.C., 2000. Depositional Sequence Response to Foreland Deformation in the Upper Cretaceous of the Southern Pyrenees, Spain. American Association of Petroleum Geologists (AAPG) Bulletin, 84, 566-587. DOI: https://doi.org/10.1306/C9EBCE55-1735-11D7-8645000102C1865D

Berástegui, X., Garcia-Senz, J.M., Losantos, M., 1990. Tecto-sedimentary evolution of the Organya extensional basin (central south Pyrenean unit, Spain) during the Lower Cretaceous. Bulletin de la Societe Geologique de France VI, 251-264. DOI: https://doi.org/10.2113/gssgfbull.VI.2.251

Bond, R.M.G., McClay, K.R., 1995. Inversion of a Lower Cretaceous extensional basin, south central Pyrenees, Spain. Geological Society, London, 88 (Special Publications), 415-431. DOI: https://doi.org/10.1144/GSL.SP.1995.088.01.22

Brun, J.-P., Fort, X., 2004. Compressional salt tectonics (Angolan margin). Tectonophysics, 382, 129-150. DOI: https://doi.org/10.1016/j.tecto.2003.11.014

Carrera, N., Muñoz, J.A., Roca, E., 2009. 3D reconstruction of geological surfaces by the equivalent dip-domain method: An example from field data of the Cerro Bayo Anticline (Cordillera Oriental, NW Argentine Andes). Journal of Structural Geology, 31, 1573-1585. DOI: https://doi.org/10.1016/j.jsg.2009.08.006

Caus, E., Gómez-Garrido, A., Simó, A., Sofiano, K., 1993. Cenomanian-Turonian platform to basin integrated stratigraphy in the South Pyrenees (Spain). Cretaceous Research, 14, 531-551. DOI: https://doi.org/10.1006/cres.1993.1038

Cramez, C., Jackson, M.P.A., 2000. Superposed deformation straddling the continental-oceanic transition in deep-water Angola. Marine and Petroleum Geology, 17, 1095-1109. DOI: https://doi.org/10.1016/S0264-8172(00)00053-2

Espurt, N., Angrand, P., Teixell, A., Labaume, P., Ford, M., de Saint Blanquat, M., Chevrot, S., 2019. Crustal-scale balanced

cross-section and restorations of the Central Pyrenean belt (Nestes-Cinca transect): Highlighting the structural control of Variscan belt and Permian-Mesozoic rift systems on mountain building. Tectonophysics 764, 25-45. DOI: https://doi.org/10.1016/j.tecto.2019.04.026

Fernández, O., 2004. Reconstruction of Geological Structures in 3D: An Example from the Southern Pyrenees. PhD Thesis. Barcelona, Universitat de Barcelona, 642pp.

Fernández, O., Muñoz, J.A., Arbués, P., Falivene, O., Marzo, M., 2004. Three-dimensional reconstruction of geological surfaces: An example of growth strata and turbidite systems from the Ainsa basin (Pyrenees, Spain). Bulletin, 88, 1049-1068. DOI: https://doi.org/10.1306/02260403062

Fernandez, O., Olaiz, A., Cascone, L., Hernandez, P., de Faria, A., Tritlla, J., Ingles, M., Aida, B., Pinto, I., Rocca, R., Sanders, C., Herrá, A., Tur, N., 2020. Geophysical evidence for breakup volcanism in the Angola and Gabon passive margins. Marine and Petroleum Geology, 104-330. DOI: https://doi.org/10.1016/j.marpetgeo.2020.104330

García-Senz, J., 2002. Cuencas extensivas del Cretácico Inferior en los Pirineos centrales. Formación y subsecuente inversión. PhD Thesis. Barcelona, Universitat de Barcelona, 321pp.

García-Senz, J., López-Mir, B., Muñoz, J.A., Arbués, P., 2019a. The South Pyrenean Basin. In: Quesada, C., Oliveira, J.T. (eds.). The Geology of Iberia: A Geodynamic Approach. Switzerland, Springer Nature, 320-341.

García-Senz, J., Pedrera, A., Ayala, C., Ruiz-Constán, A., Robador, A., Rodríguez-Fernández, L.R., 2019b. Inversion of the north Iberian hyperextended margin: the role of exhumed mantle indentation during continental collision. Geological Society, London, Special Publications, SP490-2019-112. DOI: https://doi.org/10.1144/SP490-2019-112

García-Senz, J., Ramírez, J.I., 1997. Mapa geológico de España 1:50,000 Segunda serie. Hoja 213 / Pont de Suert. Instituto Geológico y Minero de España (IGME).

Garrido-Mejías, A., 1973. Estudio geológico y relación entre tectónica y sedimentación del Secundario y Terciario de la vertiente meridional pirenaica en su zona central (Provincias de Huesca y Lérida). PhD Thesis. Granada, Universidad de Granada, 395pp.

Gómez-Garrido, A., 1987. Foraminíferos planctónicos del Cretácico Superior surpirenaico. PhD Thesis. Bellaterra, Universitat Autònoma de Barcelona, 184pp.

Groshong, R.H., 2006. 3-D Structural Geology: A Practical Guide to Quantitative Surface and Subsurface Map Interpretation, Springer-Verlag, Berlin Heidelberg. DOI: https://doi.org/10.1007/978-3-540-31055-6

Hudec, M.R., Norton, I.O., Jackson, M.P.A., Peel, F.J., 2013. Jurassic evolution of the Gulf of Mexico salt basin. Bulletin, 97, 1683-1710. DOI: https://doi.org/10.1306/04011312073

Jackson, C.A.-L., Jackson, M.P.A., Hudec, M.R., 2015. Understanding the kinematics of salt-bearing passive margins: A critical test of competing hypotheses for the origin of the Albian Gap, Santos Basin, offshore Brazil. Geological Society of America Bulletin, 127, 1730-1751. DOI: https://doi.org/10.1130/B31290.1

Jammes, S., Manatschal, G., Lavier, L., Masini, E., 2009. Tectonosedimentary evolution related to extreme crustal thinning ahead of a propagating ocean: Example of the western Pyrenees. Tectonics, 28(4), TC4012. DOI: https://doi.org/10.1029/2008TC002406

Lagier, Y., 1985. Recherches sédimentologiques sur des dépôts calcaires profonds (Exemples du Crétacé supérieur des Pyrénées). Toulouse, Thèse 3ème Cycle Sciences, 217pp.

Lopez-Mir, B., 2013. Extensional salt tectonics in the Cotiella post-rift basin (south-central Pyrenees): 3D structure and evolution. PhD Thesis. Barcelona, Universitat de Barcelona, 314pp.

Lopez-Mir, B., Muñoz, J.A., García Senz, J., 2014. Restoration of basins driven by extension and salt tectonics: Example from the Cotiella Basin in the central Pyrenees. Journal of Structural Geology, 69, 147-162. DOI: https://doi.org/10.1016/j.jsg.2014.09.022

Lopez-Mir, B., Muñoz, J.A., García-Senz, J., 2015. Extensional salt tectonics in the partially inverted Cotiella post-rift basin (south-central Pyrenees): structure and evolution. International Journal of Earth Sciences (Geologische Rundschau), 104, 419-434. DOI: https://doi.org/10.1007/s00531-014-1091-9

Lopez-Mir, B., Muñoz, J.A., García-Senz, J., 2016a. 3D geometric reconstruction of Upper Cretaceous passive diapirs and salt withdrawal basins in the Cotiella Basin (southern Pyrenees). Journal of the Geological Society, 173, 616-627. DOI: https://doi.org/10.1144/jgs2016-002

Lopez-Mir, B., Muñoz, J.A., García-Senz, J., 2016b. Geology of the Cotiella thrust sheet, southern Pyrenees (Spain). Journal of Maps, 12, 323-327. DOI: https://doi.org/10.1080/17445647.2016.1211895

Martín-Chivelet, J., López-Gómez, J., Aguado, R., Arias, C., Arribas, J., Arribas, M.E., Aurell, M., Bádenas, B., Benito, M.I., Bover-Arnal, T., Casas-Sainz, A., Castro, J.M., Coruña, F., de Gea, G.A., Fornós, J.J., Fregenal-Martínez, M., García-Senz, J., Garófano, D., Gelabert, B., Giménez, J., González-Acebrón, L., Guimerà, J., Liesa, C.L., Mas, R., Meléndez, N., Molina, J.M., Muñoz, J.A., Navarrete, R., Nebot, M., Nieto, L.M., Omodeo-Salé, S., Pedrera, A., Peropadre, C., Quijada, I.E., Quijano, M.L., Reolid, M., Robador, A., Rodríguez-López, J.P., Rodríguez-Perea, A., Rosales, I., Ruiz-Ortiz, P.A., Sàbat, F., Salas, R., Soria, A.R., Suarez-Gonzalez, P., Vilas, L., 2019. The Late Jurassic–Early Cretaceous Rifting, In: Quesada, C., Oliveira, J.T. (eds.). The Geology of Iberia: A Geodynamic Approach: Volume 3: The Alpine Cycle, Regional Geology Reviews. Springer International Publishing, Cham, 169-249. DOI: https://doi.org/10.1007/978-3-030-11295-0_5

Martinez-Peña, M., Casas-Sainz, A., 2003. Cretaceous–Tertiary tectonic inversion of the Cotiella Basin (southern Pyrenees, Spain). International Journal of Earth Sciences (Geologische Rundschau), 92, 99-113. DOI: https://doi.org/10.1007/s00531-002-0283-x

McClay, K., Muñoz, J.-A., García-Senz, J., 2004. Extensional salt tectonics in a contractional orogen: A newly identified tectonic event in the Spanish Pyrenees. Geology, 32, 737-740. DOI: https://doi.org/10.1130/G20565.1

Mencos, J., Carrera, N., Muñoz, J.A., 2015. Influence of rift basin geometry on the subsequent postrift sedimentation and basin inversion: The Organyà Basin and the Bóixols thrust sheet (south central Pyrenees). Tectonics, 34, 1452-1474. DOI: https://doi.org/10.1002/2014TC003692

Mey, P.H.W., Nagtegaal, P.J.C., Roberti, K.J., Hartevelt, J.J.A., 1968. Lithostratigraphic subdivision of Post-Hercynian deposits in the South-Central Pyrenees, Spain. Leidse Geologische Mededelingen, 41, 221-228.

Misch, P., 1934. La estructura tectónica de la región central de los Pirineos meridionales. Publicaciones extranjeras sobre la geología de España, IV, 178pp.

Mohriak, W.U., Szatmari, P., Anjos, S., 2012. Salt: geology and tectonics of selected Brazilian basins in their global context. Geological Society, London, 363 (Special Publications), 131-158. DOI: https://doi.org/10.1144/SP363.7

Muñoz, J.A., 2002. Alpine Tectonics I, the Pyrenees. The Geology of Spain. In: Gibbons, W., Moreno, T. (eds.). Geological Society London, 370-385.

Muñoz, J.A., 1992. Evolution of a continental collision belt: ECORS-Pyrenees crustal balanced cross-section. In: McClay, K.R. (ed.). Thrust Tectonics. Dordrecht, Springer Netherlands, 235-246. DOI: https://doi.org/10.1007/978-94-011-3066-0_21

Muñoz, J.A., Beamud, E., Fernández, O., Arbués, P., Dinarès-Turell, J., Poblet, J., 2013. The Ainsa Fold and thrust oblique zone of the central Pyrenees: Kinematics of a curved contractional system from paleomagnetic and structural data: PALEOMAGNETISM IN S PYRENEES. Tectonics, 32, 1142-1175. DOI: https://doi.org/10.1002/tect.20070

Muñoz, J.A., García-Senz, J., Fernandez, O., Arbués, P., Marzo, M., Roca, E., 2000. Estructura geológica y estratigrafía de la Cuenca de Graus (Pirineo Central). Estado actual del conocimiento y sistemas de hidrocarburos. Internal report for REPSOL-YPF, Geomodels Research Center (Universitat de Barcelona), 45pp.

Muñoz, J.A., Mencos, J., Roca, E., Carrera, N., Gratacós, O., Ferrer, O., Fernández, O., 2018. The structure of the South-Central-Pyrenean fold and thrust belt as constrained by subsurface data. Geologica Acta, 16(4), 439-460. DOI: https://doi.org/10.1344/GeologicaActa2018.16.4.7

Nagtegaal, P.J.C., 1972. Depositional history and clay minerals of the Upper Cretaceous basin in the South-Central Pyrenees, Spain. Leidse Geologische Mededelingen, 47, 251-275.

Papón, J.P., 1969. Etude géologique du massif montagneux du Turbon (Pyrénées aragonaises - Espagne). Bulletin de la Société d'Histoire Naturelle de Toulouse, 105, 191-211.

Ramos, A., Fernández, O., Muñoz, J.A., Terrinha, P., 2017a. Impact of basin structure and evaporite distribution on salt tectonics in the Algarve Basin, Southwest Iberian margin. Marine and Petroleum Geology, 88, 961-984. DOI: https://doi.org/10.1016/j.marpetgeo.2017.09.028

Ramos, A., Fernández, O., Terrinha, P., Muñoz, J.A., 2017b. Neogene to recent contraction and basin inversion along the Nubia-Iberia boundary in SW Iberia. Tectonics, 36, 257-286. DOI: https://doi.org/10.1002/2016TC004262

Ramos, A., Fernández, O., Terrinha, P., Muñoz, J.A., Arnaiz, Á., 2020. Paleogeographic evolution of a segmented oblique passive margin: the case of the SW Iberian margin. International Journal of Earth Sciences (Geologische Rundschau), 109, 1871-1895. DOI: https://doi.org/10.1007/s00531-020-01878-w

Robador, A., Zamorano, M., 1999. Mapa geológico de España 1:50,000 Segunda serie. Hoja 212 /Campo. Instituto Geológico y Minero de España (IGME).

Roca, E., Muñoz, J.A., Ferrer, O., Ellouz, N., 2011. The role of the Bay of Biscay Mesozoic extensional structure in the configuration of the Pyrenean orogen: Constraints from the MARCONI deep seismic reflection survey. Tectonics, 30(2). DOI: https://doi.org/10.1029/2010TC002735

Salazar, J.A., Knapp, J.H., Knapp, C.C., Pyles, D.R., 2014. Salt tectonics and Pliocene stratigraphic framework at MC-118, Gulf of Mexico: An integrated approach with application to deep-water confined structures in salt basins. Marine and Petroleum Geology, 50, 51-67. DOI: https://doi.org/10.1016/j.marpetgeo.2013.11.003

Saura, E., Ardèvol i Oró, L., Teixell, A., Vergés, J., 2016. Rising and falling diapirs, shifting depocenters, and flap overturning in the Cretaceous Sopeira and Sant Gervàs subbasins (Ribagorça Basin, southern Pyrenees): Southern Pyrenees Cretaceous Diapirism. Tectonics, 35, 638-662. DOI: https://doi.org/10.1002/2015TC004001

Séguret, M., 1972. Étude tectonique des nappes et séries décollées de la parteie centrale du versant sur des Pyrénées, Publications USTELA, Montpellier, Série Géologie Structurale nº 2, 155pp.

Snidero, M., Amilibia, A., Gratacos, O., Blanc, E.J.-P., Muñoz, J.A., 2011. The 3D reconstruction of geological structures based on remote sensing data: example from the Anaran anticline, Lurestan province, Zagros fold and thrust belt, Iran. Journal of the Geological Society, 168, 769-782. DOI: https://doi.org/10.1144/0016-76492010-107

Souquet, P., 1967. Le Crétacé supérieur sud-pyrénéen en Catalogne, Aragon et Navarre. PhD Thesis. Toulouse, University of Toulouse, 529pp.

Tari, G., Molnar, J., Ashton, P., 2003. Examples of salt tectonics from West Africa: a comparative approach. Geological Society, London, 207 (Special Publications), 85-104. DOI: https://doi.org/10.1144/GSL.SP.2003.207.5

Tavani, S., Balsamo, F., Granado, P., 2018. Petroleum system in supra-salt strata of extensional forced-folds: A case-study from the Basque-Cantabrian basin (Spain). Marine and Petroleum Geology, 96, 315-330. DOI: https://doi.org/10.1016/j.marpetgeo.2018.06.008

Tugend, J., Manatschal, G., Kusznir, N.J., Masini, E., Mohn, G., Thinon, I., 2014. Formation and deformation of hyperextended rift systems: Insights from rift domain mapping in the Bay of

Biscay-Pyrenees. Tectonics, 33, 1239-1276. DOI: https://doi.org/10.1002/2014TC003529

Turner, J.P., 1999. Detachment faulting and petroleum prospectivity in the Rio Muni Basin, Equatorial Guinea, West Africa. Geological Society, London, 153 (Special Publications), 303-320. DOI: https://doi.org/10.1144/GSL.SP.1999.153.01.19

van Hoorn, B., 1970. Sedimentology and paleogeography of an Upper Cretaceous turbidite basin in the South-Central Pyrenees, Spain. Leidse Geologische Mededelingen, 45, 73-154.

Vergés, J., García-Senz, J., 2001. Mesozoic evolution and Cainozoic inversion of the Pyrenean Rift. In: Ziegler, P.A., Cavazza, W., Roberston, A.H.F., Crasquin-Soleau, S. (eds.). Peri-Tethys Memoir 6: Peri-Tethyan Rift/Wrench Basins and Passive Margins. Mémoires du Muséum national d'histoire naturelle, 186, 187-212.

Manuscript received June 2020;
revision accepted November 2020;
published Online December 2020.